TISSUE ENGINEERING: Part C
Volume 17, Number 7, 2011

DOI: 10.1089/ten.tec.2010.0467

# Chitosan Scaffolds Containing Hyaluronic Acid for Cartilage Tissue Engineering

Clara R. Correia, M.Sc.,[1,2] Liliana S. Moreira-Teixeira, M.Sc.,[3] Lorenzo Moroni, Ph.D.,[3] Rui L. Reis, Ph.D.,[1,2] Clemens A. van Blitterswijk, Ph.D.,[3] Marcel Karperien, Ph.D.,[3] and João F. Mano, Ph.D.[1,2]

Scaffolds derived from natural polysaccharides are very promising in tissue engineering applications and regenerative medicine, as they resemble glycosaminoglycans in the extracellular matrix (ECM). In this study, we have prepared freeze-dried composite scaffolds of chitosan (CHT) and hyaluronic acid (HA) in different weight ratios containing either no HA (control) or 1%, 5%, or 10% of HA. We hypothesized that HA could enhance structural and biological properties of CHT scaffolds. To test this hypothesis, physicochemical and biological properties of CHT/HA scaffolds were evaluated. Scanning electron microscopy micrographs, mechanical properties, swelling tests, enzymatic degradation, and Fourier transform infrared (FTIR) chemical maps were performed. To test the ability of the CHT/HA scaffolds to support chondrocyte adhesion and proliferation, live–dead and MTT assays were performed. Results showed that CHT/HA composite scaffolds are noncytotoxic and promote cell adhesion. ECM formation was further evaluated with safranin-O and alcian blue staining methods, and glycosaminoglycan and DNA quantifications were performed. The incorporation of HA enhanced cartilage ECM production. CHT/5HA had a better pore network configuration and exhibited enhanced ECM cartilage formation. On the basis of our results, we believe that CHT/HA composite matrixes have potential use in cartilage repair.

## Introduction

Cartilage damage frequently occurs because of sports or progressive ageing. Once damaged, cartilage cannot be spontaneously repaired because of its avascularity and low cellular mitotic activity.[1] A range of clinical options emerged to repair focal lesions and damage to the articular surface. These approaches may reduce pain and increase mobility, but only to a limited extent and over a short-term period.[2,3] Current strategies are not able to fully restore the native structure of cartilage, which raises concerns about the long-term performance of repaired cartilage.[4] These partial successes lead to significant research efforts to develop tissue engineering therapies for cartilage repair.

The main challenge for cartilage tissue engineering is the chondrocytes massive transition into fibroblastic cells during the *in vitro* culture process. Those dedifferentiated cells form fibrocartilage instead of hyaline cartilage.[5] Additionally, chondrocytes availability is limited because of the size of biopsies that can be collected from the patient's own tissue, without causing the risk of morbidity of the site of explant. Moreover, the development of biodegradable polymers to perform the role of a temporary matrix is an important factor in the success of cell transplantation.[6,7]

Extracellular matrices (ECMs) provide a microenvironment for cells to maintain homeostasis and to retain the required differentiated state for specific tissues.[8] Among the many different ECM molecules, hyaluronic acid (HA) is the main glycosaminoglycan (GAG) in the mesenchyme during the early stage of chondrogenesis.[9,10] In addition, HA is known to influence chondrocytes by triggering a sophisticated signaling pathway leading to enhancement of cellular functions.[11,12] However, the concentration of HA must be confined to a relatively low amount, as concentrations may reduce cell adhesion because of its negative charge.[13] This disadvantage can be overcome by combining HA with positively charged polycations such as chitosan (CHT).[14] CHT, a partially deacetylated derivative from chitin, has the ability to interact with negatively charged molecules.[15] Because of its biocompatibility and biodegradability, CHT has been widely applied in tissue engineering strategies.[16–19] Additionally, CHT is structurally similar to various GAGs

[1]3B's Research Group—Biomaterials, Biodegradables, and Biomimetics, Headquarters of the European Institute of Excellence on Tissue Engineering and Regenerative Medicine, University of Minho, Guimarães, Portugal.
[2]PT Associated Laboratory, IBB—Institute for Biotechnology and Bioengineering, Guimarães, Portugal.
[3]Department of Tissue Regeneration, MIRA—Institute for Biomedical Technology and Technical Medicine, Twente University, Enschede, The Netherlands.

found in articular cartilage.[20] Combining the advantages of both polysaccharides, CHT/HA scaffolds can be suitable candidates for cartilage tissue regeneration. The blend would be stabilized by an ionic interaction between the positively charged CHT and the negatively charged HA.

CHT has been already conjugated with HA to obtain a biomimetic matrix for chondrocytes.[16,21–24] Yamane *et al.*[22] developed CHT-based HA polymer fibers by the wetspinning method. In the hybrid fibers, chondrocyte adhesion, proliferation, and also the synthesis of aggrecan and type II collagen were significantly higher when compared with CHT fibers. Hsu *et al.*[24] studied CHT–alginate–hyaluronan scaffolds, with or without covalent attachment, with RGD-containing protein. The cell-seeded scaffolds showed neocartilage formation *in vitro* in the presence or absence of RGD. Tan *et al.*[21] demonstrated that CHT-HA hydrogels allowed cell survivor, and cells retained the chondrogenic morphology.

The reported studies are focused on the superior biological effects that HA could provide, and its incorporation has not been studied in terms of physicochemical effects. Additionally, to our knowledge, the effect of varying the ratio between CHT and HA, and consequently, its influence in terms of both physicochemical and biological properties, has not been yet reported. On the other hand, because of HA high water uptake and the lack of mechanical strength provided by natural polymers, the existing strategies combining CHT and HA for cartilage tissue engineering are very limited and usually consist in hydrogels.[21,25] However, these hydrogels do not have the required mechanical strength to maintain the initial shape of the implanted scaffold. Consequently, they cannot be transplanted into large cartilaginous lesions in advanced degenerative diseases, such as osteoarthritis and rheumatoid arthritis. Moreover, the existing CHT/HA blends are usually used to produce scaffolds by techniques more complex than the freeze-drying method, in which further research is needed to determine the adequate shape, pore size, and mechanical properties of a three-dimensional fabrication for cartilage TE.

The aim of this work was to prepare a new class of hybrid scaffolds composed of CHT as a framework containing low concentrations of HA to mimic cartilage ECM composition. The application of HA as a component of the cartilage scaffold biomaterial could be a reasonable approach for enhancing chondrogenesis. We hypothesized that HA could provide superior effects on the formation and structural and biological properties of CHT scaffolds, by providing a suitable microenvironment where chondrocytes may produce a cartilage-specific matrix for cartilage regeneration. To test this hypothesis, HA was added to CHT solution in a final polymer concentration of 2% (w/v) to prepare three-dimensional scaffolds by freeze-drying method.[19] Using this method, porous scaffolds are easily prepared with controllable pore size, uniform pore distribution, and functional features. Four types of scaffolds were obtained containing either no HA (control, CHT) or 1% (CHT/1HA), 5% (CHT/5HA), and 10% of HA (CHT/10HA). The physicochemical properties and biological behavior of the developed scaffolds were evaluated to study the HA influence in the CHT scaffolds in different parameters, including pore size and geometry, mechanical properties, and cartilage ECM production.

## Materials and Methods

### Materials

Medium-molecular-weight CHT ($M_w$: 190,000–310,000, 75%–85% deacetylation degree, viscosity: 200–800 cps) and HA (#81, Lot Dev 00453, $M_w$: 1.8 million) were purchased from Sigma-Aldrich. Before being used, CHT was purified by recrystallization. CHT was dissolved in 1% (w/v) acetic acid solution and then filtered under vacuum through porous membranes (Whatman ashes filter paper, 20–25 μm) into a Buckner flask. By adding a solution of sodium hydroxide, the pH of the solution was adjusted to 8, resulting in flocculation due to deprotonation and insolubility of the polymer at neutral pH. The polymer solution was then neutralized until the pH was equal to that of distilled water. Samples were frozen at −80°C and lyophilized. Lysozyme from chicken egg white (lyophilized powder, ~100,000 U/mg, stored at 4°C) and hyaluronidase from bovine tests (Type VIII, 300 U/mg, stored at −20°C) were purchased from Sigma-Aldrich.

### Methods

**Preparation of CHT and HA scaffolds.** CHT and HA were first separately dissolved (1%, w/v) overnight at room temperature in diluted acetic acid (1%, v/v) and subsequently mixed in different ratios (w/v) in a final polymer concentration of 2% (w/v). To obtain a cylindrical shape, the polymeric solutions were placed into plastic tubes and frozen for 1 day at −80°C. The plastic tubes were then cut into small pieces to obtain a scaffold dimension of 5 mm × Ø 6 mm. After freeze-drying, the scaffolds were neutralized with a solution of NaOH (0.1 M) and then freeze-dried again. Four types of scaffolds were obtained, containing 0% (control), 1%, 5%, or 10% of HA (CHT; CHT/1HA; CHT/5HA; and CHT/10HA, respectively).

**Physicochemical characterization.** *Morphology and pore size:* The morphology of CHT/HA scaffolds was characterized by scanning electron microscopy (SEM). The scaffolds were gold-coated using a sputter coater (Cressington) for 60 s at a current of 40 mA. Cross-sectional morphologies were viewed using a Philips XL 30 ESEM-FEG operated at 10 kV accelerating voltage. Pore size was measured using a submenu, consisting on a ruler tool, incorporated in the software of the SEM equipment. Once the overall cross-sectional images of the scaffolds were obtained, several pores (>20) were selected. In each selected pore, the ruler tool measured the diameter of the pore by measuring the distance between two points. In each cross-sectional image of the scaffolds, the average pore size was calculated.

*Fourier transform infrared spectroscopy imaging measurements:* To confirm the presence of chitosan or hyaluronic acid in the different scaffold's formulations, Fourier transform infrared (FTIR) measurements were performed using a Perkin-Elmer Spectrum Spotlight 200 FTIR Microscope System in reflectance mode. As a monochromotic light beam reaches the sample, subsequently, the light reflected is measured for different wavelengths. The reflected light at a determined wavelength is characteristic for each functional group, thus it can be identified, confirming its presence in the sample analyzed. The four scaffold formulations and a sample of pure HA were analyzed without further modifications in the range of 720–1800 $cm^{-1}$. The selected region for CHT

identification was 1650 $cm^{-1}$, which corresponds to C=O stretching of amide I.[26] The selected region for HA was 1045 $cm^{-1}$, which corresponds to C-O-C bond stretching vibration of symmetric ester band.[27,28] To obtain the chemical maps, a submenu incorporated in the software of the FTIR equipment was used. Two ranges and three colors were selected. For CHT, the range 1630–1670 $cm^{-1}$ integrates the amide I characteristic peak and it is represented in green. For HA, the range 1025–1065 $cm^{-1}$ integrates the ester characteristic peak and it is represented in red. The color yellow was selected to represent the presence of the two characteristic peaks simultaneously. Spectra were collected in continuous scan mode for sample areas of $85 \times 85\ \mu m^2$, with a spectral resolution of 16 $cm^{-1}$ by averaging 15 scans for each spectrum.

*Mechanical properties:* Mechanical compression tests of the scaffolds were performed using an INSTRON 5543 (Instron Int. Ltd.) up to 60% of strain, at room temperature. The testing machine was equipped with a 1 kN load cell and the loading rate was 2 mm/min. The compressive modulus was calculated in the initial linear section of the stress–strain curve, when the strain was lower than 10%. The mechanical properties of the scaffolds were tested in both dry and wet states. In the wet state assay, scaffolds were immersed in phosphate-buffered saline (PBS) at pH 7.4 for 24 h in a shaking water bath at 37°C to simulate *in vivo* conditions and for complete hydration. Compressive mechanical tests were performed in $n = 6$ per scaffold formulation in both assays.

*Swelling properties*: The water sorption capacity of the scaffolds was determined by swelling of freeze-dried scaffolds (with known weights) in PBS (Gibco) at pH 7.4 for 3 days at 37°C. The swollen scaffolds were removed at predetermined time intervals (15 min, 30 min, 1 h, 2 h, 4 h, 6 h, 8 h, 24 h, 2 days, and 3 days) and immediately weighed with an analytical balance (Scaltec) after the removal of excess of water by keeping the surfaces on a filter paper (Whatman Pergamyn Paper, 100 × 100 mm). The swelling ratio (SR) was calculated using the following equation (1):

$$SR = (W_w - W_d)/W_d \quad (1)$$

where $W_w$ and $W_d$ are the weights of the scaffolds at the swelling state and the dry state, respectively.

*Enzymatic degradation*: CHT/HA scaffolds were placed at pH 7.4 in PBS (control) or at pH 7.11 in an enzymatic solution containing 2 mg/mL of lysozyme[29] and 0.33 mg/mL of hyaluronidase[30] in a shaking water bath at 37°C. The medium was replaced every third day. At predetermined time intervals (7 and 14 days), scaffolds were taken from the solutions and washed with distilled water three times to remove salts. The weight was measured after the scaffolds were immersed in 100% ethanol for 2 h and dried for 1 day at room temperature. The percentage weight loss (%WL) of scaffolds was calculated according to the following equation (2):

$$\%WL = [(W_i - W_f)/W_i] \times 100\% \quad (2)$$

where $W_i$ is the initial dry weight of scaffold and $W_f$ is the weight of the dry scaffold after incubation in the PBS or enzymatic solution.

Bovine articular chondrocyte culture. Bovine articular chondrocytes were isolated from freshly collected cartilage from a calf knee through enzymatic digestion, under sterile conditions. Briefly, cartilage was minced in small pieces, which were incubated overnight in Dulbecco's modified Eagle's medium (DMEM) with 0.2% collagenase II (Worthington). Afterward, cells were washed with PBS (Gibco) and resuspended in chondrocyte proliferation medium containing DMEM high glucose (Invitrogen), fetal bovine serum (10%; Sigma-Aldrich), nonessential amino acids (0.1 mM; Sigma-Aldrich), penicillin/streptomycin (100 U/100 μg/mL; Invitrogen), proline (0.4 mM; Sigma-Aldrich), and Asap (0.2 mM; Invitrogen). Ultimately, cells were seeded in plastic tissue culture flasks and incubated in a humidified atmosphere with 5% $CO_2$ at 37°C. Adherent chondrocytes were expanded and the medium was changed every third day, until the cells achieved 80% confluence.

Prior to cell seeding, the scaffolds were sterilized with 70% (v/v) ethanol for 2 h, rinsed three times in distilled water, and then immersed in PBS for 2 days. The seeding was performed by injection of a cell suspension, on which the cell concentration was adjusted to $0.5 \times 10^6$ cells in 20 μL of medium (per scaffold). After incubation for 4 h at 37°C in a 5% $CO_2$ atmosphere incubator, chondrocyte proliferation medium or chondrocyte differentiation medium [DMEM, 2 mM glutamax (Gibco), 0.2 mM Asap (Invitrogen), 100 μg/mL penicillin/streptomycin, 0.4 mM proline (Sigma-Aldrich), 100 μg/mL sodium pyruvate (Sigma-Aldrich), and 50 mg/mL ITS+premix (BD biosciences]. Immediately before use, 10 ng/mL TGF-β3 (R&D Systems) and 0.1 μM dexamethasone (Sigma-Aldrich) were added to the seeded scaffolds, according to the type of assay performed.

Biological assays. To analyze cell viability, proliferation, and adhesion of CHT/HA scaffolds, articular bovine chondrocytes were seeded by injection at passage 3 in proliferation medium. Live/dead and MTT assays were performed at 1, 3, 7, 14, and 21 days, according to manufacturer's specifications, and scaffolds were further observed by SEM. To evaluate the chondrogenic phenotype maintenance, articular bovine chondrocytes were seeded by injection at passage 1 in differentiation medium. Safranin-O and alcian blue staining methods, quantitative GAG and DNA assays, and SEM observation were performed. Chondrocyte medium was changed every third day to maintain an adequate supply of cell nutrients.

*Live/dead assay:* Scaffolds were deposited in a 48-well plate. To perform this assay, chondrocyte proliferation medium was aspirated from the wells and the seeded scaffolds were incubated with ethidium homodimer-1 (6 μM) and calcein-AM (4 mM) (Invitrogen) for 30 min in the dark at 37°C in a 5% $CO_2$ atmosphere incubator. Scaffolds were immediately examined in an inverted fluorescent microscope (Nikon Eclipse E600) using an FITC/Texas Red Filter. The images were captured using a color camera (Nikon FDX-35) and the QCapture software. Calcein-AM is enzymatically converted, producing fluorescent living cells, as live cells have intracellular esterase activity. Ethidium homodimer-1 is only able to enter dead cells, and after binding to nuclei acids, a red fluorescent signal is produced.

*MTT assay*: Scaffolds were deposited in a 48-well plate and incubated with 1 mL of chondrocytes proliferation medium and 20 μL MTT solution (5 mg/mL; Gibco) per well for 2 h at 37°C in a 5% $CO_2$ atmosphere incubator. MTT is a pale

yellow substrate, which is reduced by living cells to formazan, which stains dark purple. This process requires active mitochondria and is thus an accurate measure of the metabolic activity of cells in a culture. At the referred time intervals, MTT solution was added to each well. During this period, viable cells could reduce the MTT formazan. Images were captured using a color camera (Nikon SMZ-10A) and the MATRIX Vison SRGB 32Bit software.

*SEM observation*: Chondrocytes adhesion on scaffolds was analyzed by SEM ($n=2$). CHT/HA scaffolds were immersed in 10% (v/v) formalin overnight at 4°C. Specimens were then dehydrated using sequential ethanol series (70%, 80%, 90%, 96%, and 100% (v/v), 1 h in each, and critical point dried using a Balzers CPD 030 machine. The scaffolds were gold-sputtered as previously described for further observation by SEM operated at 10 kV accelerating voltage.

*Histology*: Safranin-O and alcian blue staining methods were used to analyze cartilage tissue formation. Scaffolds were washed with PBS, fixed overnight in 10% formalin, and then dehydrated using sequential ethanol series [70%, 80%, 90%, 96%, and 100% (v/v), 1 h in each]. Once dehydrated, they were incubated in butanol overnight and then in a solution containing butanol and paraffin (50:50) for 8 h. Ultimately, the scaffolds were embedded in paraffin and 5-μm-thick sections were cut using a microtome. After deparaffinization with xylene and rehydration using a graded ethanol series [from 100% to 70% (v/v)], the samples were stained. For safranin-O staining, sections were counter stained with hematoxylin (Sigma-Aldrich) and fast green (Merk) to visualize cells and cell nuclei, respectively, and safranin-O (Sigma-Aldrich) for visualization of GAGs in red. For alcian blue staining, sections were stained with alcian blue solution (1% in acetic acid) for 30 min to visualize extracellular GAGs in blue. After the washing steps, the samples were counterstained with nuclear fast red for 5 min. Slides were assembled with resinous medium and mounted slides were examined under a light microscope (Nikon Eclipse E600). Representative images were captured using a digital camera (Nikon FDX-35) and QCapture software. Each assay was performed at either 1, 14, 21, and 35 days of culture in duplicate ($n=2$ per scaffold formulation).

*Quantitative GAG and DNA assays*: CHT/HA scaffolds were washed with PBS and frozen at −80°C for quantitative analysis of GAG expression and cell number. Subsequently, they were digested with 1 mg/mL proteinase K (Sigma-Aldrich) in Tris/EDTA buffer (pH 7.6) containing 18.5 μg/mL iodoacetamide and 1 μg/mL pepstatin A (Sigma-Aldrich) for 20 h at 56°C. GAG content was spectrophotometrically determined with DMMB (Sigma-Aldrich) staining in PBE buffer [PBS containing 14.2 g/L $Na_2HPO_4$ and 3.72 g/L $Na_2EDTA$ (pH 6.5)] with a monochromatic microplate reader (TECAN Safire 2) at an absorbance of 520 nm. The standard curve for the GAG analysis was generated using chondroitin sulfate A (Sigma-Aldrich). Quantification of total DNA was determined with the CyQuant DNA kit, according to the manufacturer's description (Molecular Probes), using a fluorescent plate reader (emission: 520 nm; excitation: 480 nm; Perkin-Elmer). The standard curve for DNA analysis was generated with λ DNA provided with the CyQuant DNA kit. The assays were performed at 1, 14, 21, and 35 days of culture.

Statistical analysis. Each experiment was carried out in triplicate unless otherwise specified. All results are presented as mean ± standard deviation (SD). The experimental data were analyzed using single-factor analysis of variance technique to assess the statistical significance of results. Statistical significance was set at a $p$-value of $\leq 0.05$ ($^{*}$) or $\leq 0.01$ ($^{**}$).

## Results and Discussion

### *Physicochemical characterization of CHT and HA scaffolds*

Scaffolds preparation and microstructure observation. Concentrations of HA-based scaffolds are usually limited to 2% (w/v), or less, because higher concentrations

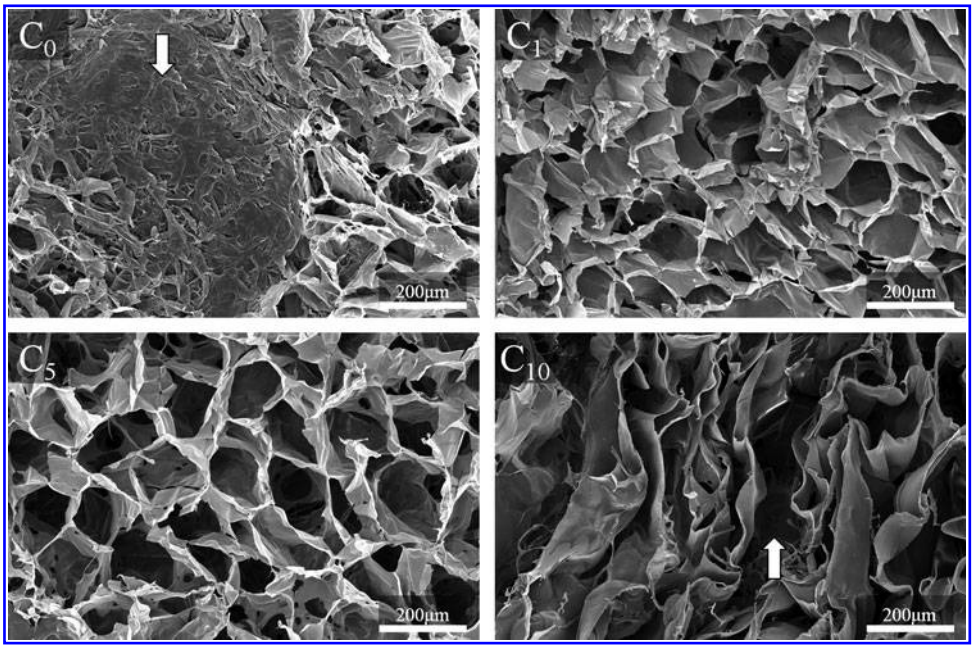


**FIG. 1.** SEM micrographs for cross section (C) of the chitosan (CHT) and hyaluronic acid (HA) scaffolds prepared, using different ratios of CHT and HA ($n=3$). The subscripts indicate the percentage of HA (0%, 1%, 5%, and 10%). $C_0$ arrow evidences the sheet-like areas of CHT scaffolds. $C_{10}$ arrow shows the irregular pore geometry of CHT/10HA scaffolds. Original magnification is ×100 and the scale bar represents 200 μm. SEM, scanning electron microscopy.

Table 1. Pore Size (μm) and Compressive Modulus (kPa) of the Chitosan/Hyaluronic Acid Scaffolds Prepared with Different Amounts of Hyaluronic Acid in Dry and Wet States

| *Sample code* | *Chitosan (% wt)* | *Hyaluronic acid (% wt)* | *Pore size (μm)* | *Compressive modulus in dry state (kPa)* | *Compressive modulus in wet state (kPa)* |
|---|---|---|---|---|---|
| CHT | 100 | 0 | 55.80 ± 10.04 | 291.03 ± 82.73 | 2.84 ± 0.41 |
| CHT/1HA | 99 | 1 | 77.40 ± 15.01 | 144.33 ± 28.32 | 2.43 ± 0.07 |
| CHT/5HA | 95 | 5 | 97.43 ± 6.56 | 144.00 ± 25.68 | 2.30 ± 0.06 |
| CHT/10HA | 90 | 10 | 148.73 ± 99.24 | 40.73 ± 18.31 | 1.21 ± 0.47 |

Values are reported as mean ± SD.

are too viscous for adequate mixing.[31] The morphologies of the scaffolds were investigated based on different ratios between CHT and HA. To characterize the microstructure morphology of CHT and HA scaffolds, cross-sectional SEM images were obtained (Fig. 1). CHT scaffolds showed a closed network pore configuration with sheet-like areas (arrow in Fig. $1C_0$). In contrast, CHT/1HA and CHT/5HA scaffolds showed a more open network structure. These two formulations had high porosity and uniformly distributed pore structures. In CHT/10HA scaffolds, pore geometry was very irregular with closed or oversized collapsed pores (arrow in Fig. $1C_{10}$). This influence on porosity and pore structure when HA was incorporated in scaffolds of polycationic polymers was also found by Ren *et al.*[13] The differences between the pore architecture are at least partially related to the homogeneity of the polymeric solution, that is, how well are the two polymers mixed and dispersed in the solution. As CHT and HA have an opposite charge, an ionic bond between the carboxyl groups of HA and the amino groups of CHT is expected.[15] As the concentration of HA increased in the CHT/HA formulation, the solution became more opaque. The incorporation of HA up to a concentration of 5% in a CHT solution yielded a well-dispersed colloidal suspension. CHT/5HA suspension was stable, indicating the formation of submicrometer complexes. In contrast, higher concentrations of HA jeopardized efficient mixture of both polymers, resulting in white precipitates. These precipitates tended to aggregate and, consequently, after freeze-drying, resulted in a nonuniform pore geometry (Fig. $1C_{10}$). Mao *et al.*[32] also studied CHT and HA blends and correlated the formation of white precipitates with the high density of carboxyl groups in HA and amino groups in CHT.

Pore size increased with concentrations of HA in CHT scaffolds (Table 1). Fan *et al.*[31] reported the same influence of HA on scaffold pore size. CHT/10HA also exhibited the highest standard deviation in pore sizes because of the nonuniform pore geometry. The open pore network and a range in pore size between ~77 and 97 μm, as observed in CHT/1HA and CHT/5HA scaffolds, rendered these scaffolds appropriate for cellular infiltration. Particularly, we hypothesize that articular bovine chondrocytes can be incorporated into the aforementioned scaffolds.

Fourier transform infrared spectroscopy imaging measurements. FTIR measurements (Fig. 2) confirmed the presence of CHT and HA in all CHT/HA scaffolds. Characteristic peaks of both polymers (Fig. 2a) were found, namely a distinct band at 1650 $cm^{-1}$ (amide I) and at 1580 $cm^{-1}$ (amide II).[26] The ester group (1045 $cm^{-1}$), a HA characteristic peak, is the main difference between the two spectra. The referred characteristic peaks were also found in all CHT/HA scaffolds spectra (Fig. 2b). Particularly, CHT/10HA had a notable higher intensity in the ester peak, as it is the formulation with higher amount of HA.

The homogeneity of the CHT/HA blends was investigated by FTIR mapping (Fig. 3). As expected, chemical maps of CHT scaffolds (Fig. 3a) and pure HA (Fig. 3b) only showed the selected color for the pure materials (green and red, respectively). As showed in Figure 3d, CHT/5HA scaffolds had an improved polymer mixture, in which the two polymers were well dispersed in the length scale ana-

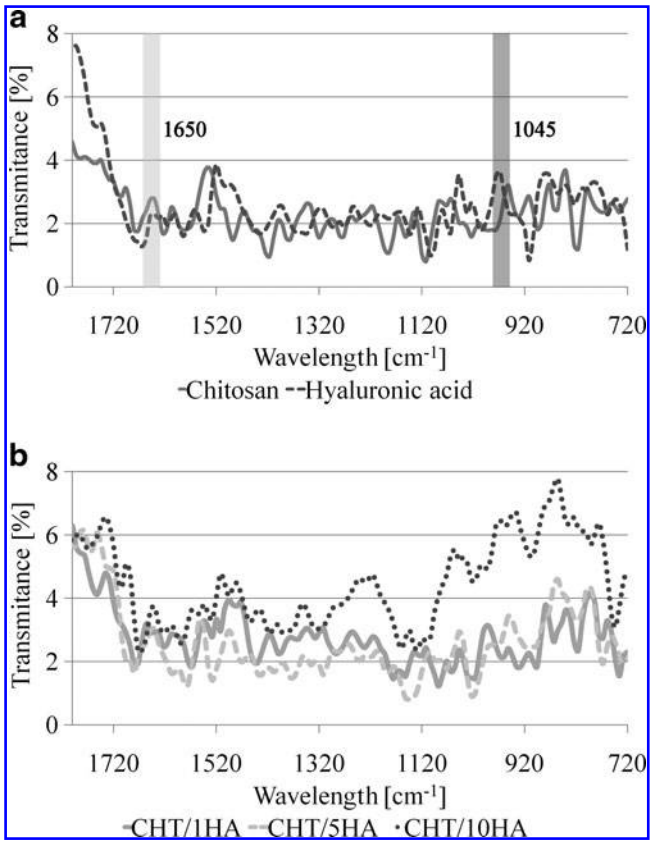


**FIG. 2.** Fourier transform infrared (FTIR) spectra of **(a)** CHT scaffolds (solid line) and pure HA (dashed line) and of **(b)** CHT/1HA (solid line), CHT/5HA (dashed line), and CHT/10HA (dotted line) scaffolds. The rectangles present at Figure 2a indicate the chosen regions for the integration procedure used to obtain the images of Figure 3, each one centered at the selected characteristic peak of chitosan (1670 $cm^{-1}$) or HA (1045 $cm^{-1}$).

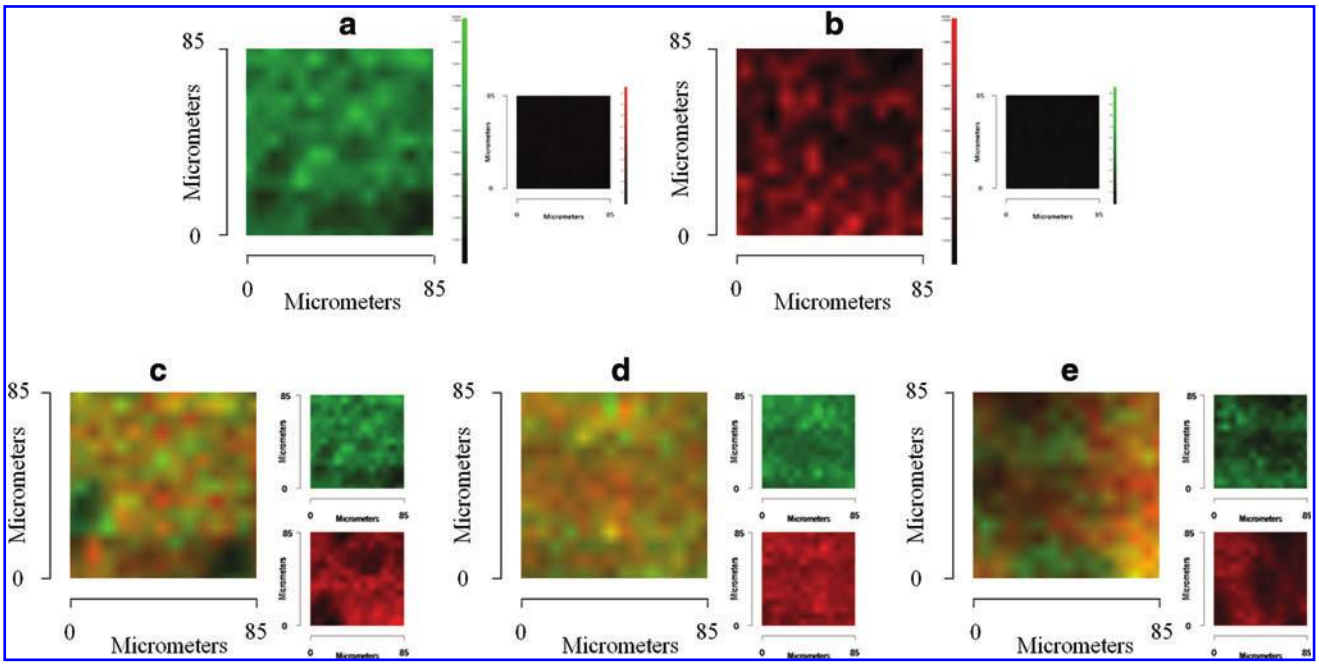


**FIG. 3.** Chemical maps obtained by FTIR microscopy of the cross sections of the scaffolds and pure HA: **(a)** CHT, **(b)** HA, **(c)** CHT/1HA, **(d)** CHT/5HA, and **(e)** CHT/10HA. Green indicates the presence of CHT and red indicates the presence of HA. The inset images individualize the presence of the pure polymers in the blends. The inset images next to **(a)** and **(b)** represent the images control for HA and CHT, respectively. Color images available online at www.liebertonline.com/tec

lyzed (tens of microns). On the other hand, in CHT/10HA scaffolds the quality of the blend was compromised. There were more green and red areas, which correspond to CHT and HA alone, respectively, and less yellow areas, which correspond to the homogeneously blended biomaterials.

Mechanical properties. The mechanical properties of the scaffolds in tissue engineering applications are of great importance because of the necessity of structural stability to withstand stresses incurred during *in vitro* culture and *in vivo* implantation.[31]

Compressive mechanical tests were performed using acellular scaffolds in dry and wet states. The compressive modulus of the scaffolds is shown in Table 1. All samples exhibited a sponge-like behavior. For both assays, the addition of HA in CHT networks reduced the mechanical strength of the scaffold, while it increased its flexibility. This behavior may essentially be due to the increase in pore size by increasing the HA concentration. It was interesting to note that CHT/1HA and CHT/5HA scaffolds had similar compressive modulus in dry and wet states, probably because of their similar pore network.

In addition to an increase in pore size, O'Brien *et al.*[33] reported a correlation between decreasing mechanical strength and nonuniform pore shape in HA-based scaffolds. This may explain the reason why CHT/10HA had a much lower compressive modulus.

In the dry state, the compressive modulus of CHT/HA scaffolds were lower but in the same order of magnitude when compared with the modulus of articular cartilage reported by Korhonen *et al.*[34] The compressive modulus in wet state was much lower compared with the dry state because of HA's ability of high water uptake. As CHT and HA are two natural polymers, this drawback in terms of mechanical strength was expected. However, the principal aim of incorporating HA into CHT scaffolds was to mimic the native cartilage ECM. The compressive modulus may further improve by the deposition of an ECM by chondrocytes in CHT/HA scaffolds.

Swelling properties. Diffusion and exchange of nutrients (e.g., oxygen) and waste throughout the entire scaffold are related to the swelling properties of the scaffolds. Both CHT and HA have an abundant number of hydrophilic groups, such as hydroxyl, amino, and carboxyl groups, which can promote water uptake in the structure.[25] The swelling ability was evaluated by soaking the scaffolds in PBS at 37°C for 3 days (Fig. 4). The ratio between CHT and HA significantly affected the scaffolds' swelling properties. In the first 2 h, all samples rapidly increased their weight. This rapid weight increase continued until 8 h. Then, the swelling ratio of all

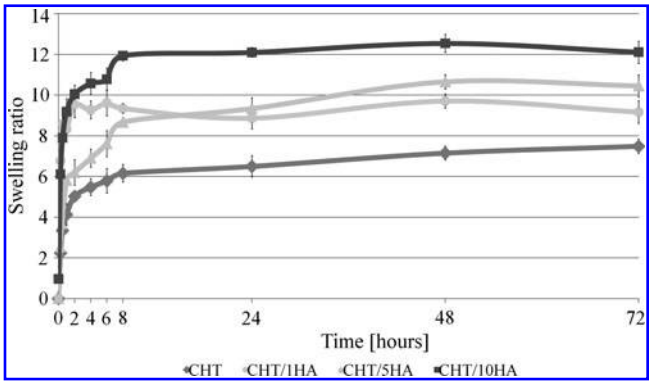


**FIG. 4.** Swelling ratio of CHT and HA scaffolds in phosphate-buffered saline at 37°C for 3 days. Values are reported as mean ± standard deviation (SD) ($n = 3$).

samples seemed to stabilize, and a slight increase could be observed with time. CHT scaffolds had the lowest values during the entire experiment, whereas CHT/10HA had the highest. CHT/1HA and CHT/5HA had similar swelling. The swelling results indicated that HA incorporation can greatly improve hydrophilicity and wetting of CHT scaffolds. Hence, scaffolds with higher content of HA showed higher values of swelling. This aspect may imply that the absorption and diffusion of solutes through the interior pores in CHT scaffolds are greatly improved by incorporation of low concentrations of HA.

In vitro enzymatic degradation. Scaffolds for tissue engineering are usually required to either degrade or be reabsorbed by the body after successful tissue regeneration. CHT/HA scaffolds were incubated in a solution with lysozyme and hyaluronidase or in a solution with PBS (control), both at 37°C for 7 and 14 days, to evaluate the weight decrease in the biopolymers due to enzymatic degradation. The weight loss percentage of scaffolds as a function of incubation time is illustrated in Figure 5.

To distinguish between enzymatic degradation and simple dissolution, we compared the weight loss of samples that had been placed in PBS (Fig. 5a) with those that had been placed in PBS supplemented with lysozyme and hyaluronidase at 7 and 14 days (Fig. 5b). According to Figure 5b, the presence of HA rendered CHT scaffolds more susceptible to enzymatic degradation, which is most likely due to higher porosity and better accessibility of cleavage sites by the enzymes. The hydrophilicity of HA also contributed to a higher degradation of CHT/HA scaffolds as it will enhance the interaction of the biomaterial with the enzymatic solution. After a high initial weight loss at day 7, the degradation rate of the samples generally appeared to slow down at day 14, which is most likely due to the gradual disappearance of hexasaccharide sequences susceptible for enzymatic degradation. The control experiment in PBS (Fig. 5a) showed that practically none of the scaffolds degrade in PBS after 14 days. The degradation of CHT has been already tested in several *in vitro* studies.[35–38] Most of these studies were, however, performed at low pH for optimal lysozyme activity. In our study, the enzymatic degradation experiments were performed at higher pH, which resembles better degradation of the scaffolds in physiological conditions. Hyaluronidase and lysozyme concentrations used in this study (0.33 and 2 mg/mL, respectively) are not representatives of their concentration *in vivo.* The largest single reservoir of hyaluronidase is the synovial fluid of diarthrodial joints (0.5–4 mg/mL).[39] Lysozyme commonly exists in various human body fluids and tissues, with concentrations ranging from 4 to 13 mg/L in serum[40] and from 450 to 1230 mg/L in tears.[41]

## In vitro *articular bovine chondrocyte culture*

Cell viability, proliferation, and adhesion studies on CHT/HA scaffolds. In a live–dead assay, all materials exhibited very good biocompatibility with hardly any detectable cell death (Fig. 6). Further, cells were metabolically active (Fig. 7) and well spread throughout the scaffolds in all formulations. The presence of increasing concentrations of HA did not influence cell loading of CHT scaffolds. This behavior is essentially due to the low capacity for cell attachment of CHT.

The cell morphology and proliferation on CHT/HA scaffolds was further studied by SEM (Fig. 8). In all scaffolds, chondrocytes were primarily localized in the superficial area at days 1 and 3 and displayed a spherical morphology (cell

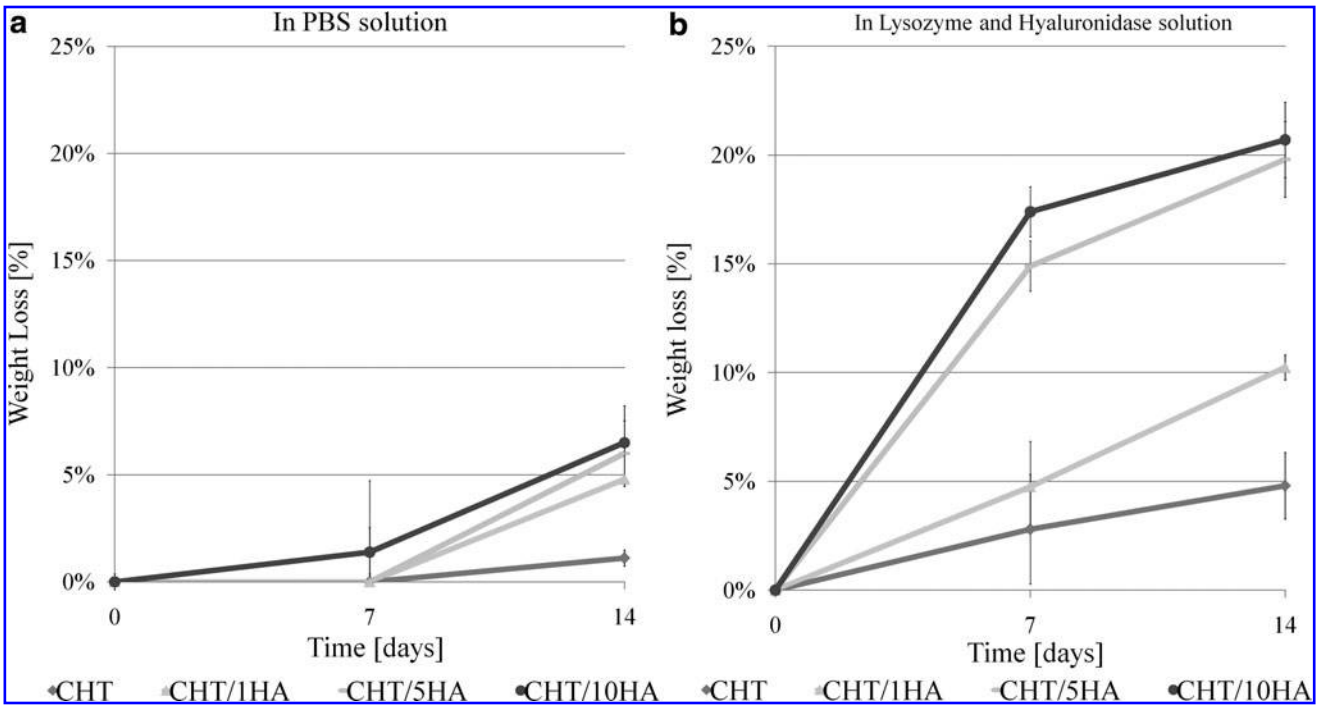


**FIG. 5.** Weight loss percentage of CHT/HA scaffolds as a function of incubation time (7 and 14 days) at 37°C. Scaffolds were embedded in **(a)** phosphate-buffered saline or **(b)** enzymatic solution containing both lysozyme and hyaluronidase. Values are reported as mean ± SD ($n = 3$).

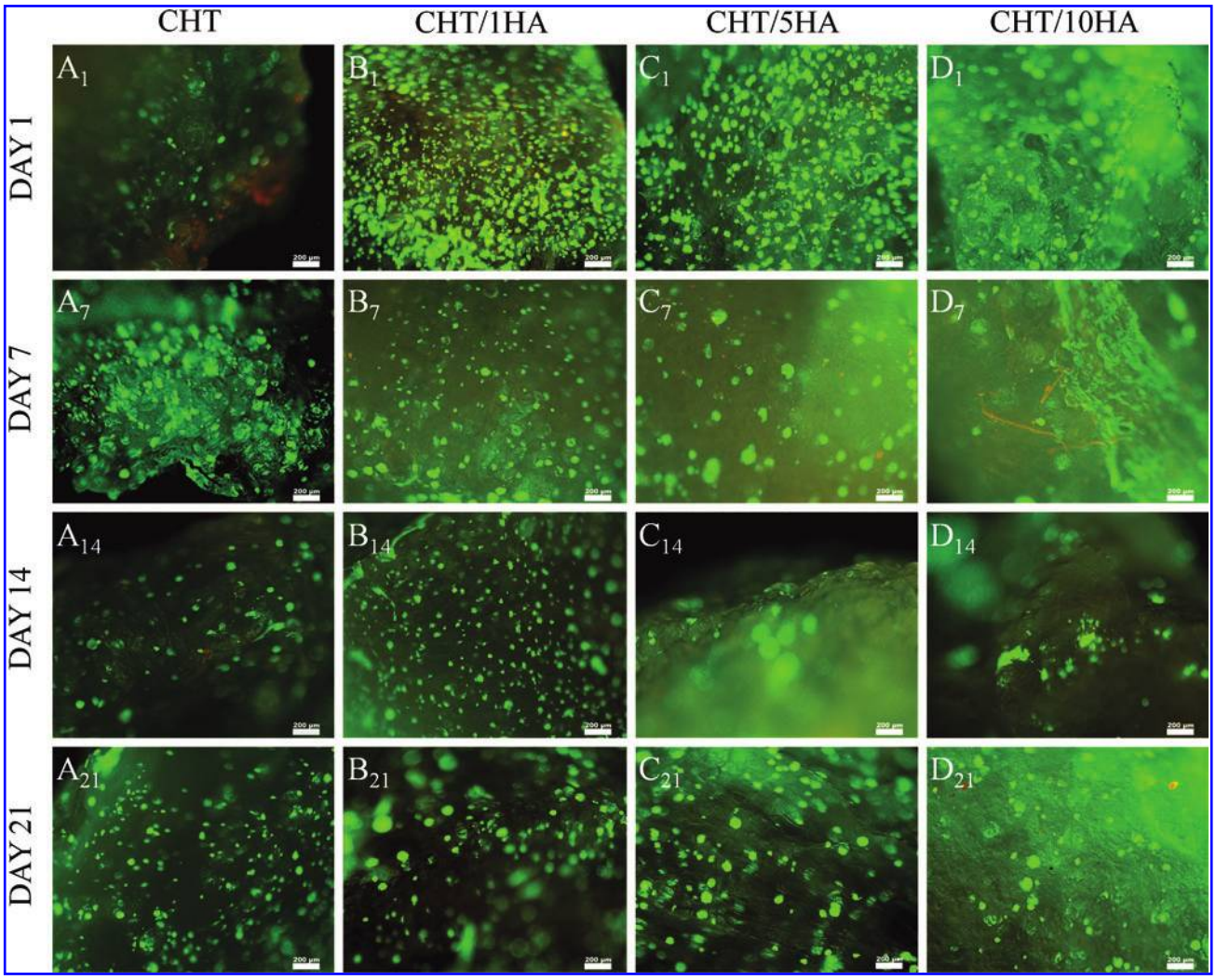


**FIG. 6.** Live–dead assay results of chondrocytes at passage 3 in proliferation medium seeded on CHT/HA scaffolds at days 1, 7, 14, and 21. Live cells were stained green by calcein and dead cells were stained red by ethidium ($n=3$). Letters **A–D** correspond to each of the four scaffold's formulations, namely CHT, CHT/1HA, CHT/5HA or CHT/10HA, respectively. The subscripts indicate the time period. Scale bar is 200 μm. Color images available online at www.liebertonline.com/tec

size diameter: ~10 μm). At day 7, a limited increase in cell number was observed but cells did not penetrate into the scaffolds. At days 14 and 21, chondrocytes seeded in CHT/5HA scaffolds significantly proliferated into the inner areas of the scaffolds. In all scaffolds, even after 21 days of culture, the cells continued to display a normal spherical morphology, as observed in native cartilage.

Maintenance of chondrogenic phenotype. The round shape of chondrocytes is an indicator of phenotype retention and is essential for matrix formation.[42] The newly formed matrix was stained with safranin-O (Fig. 9) and alcian blue (Fig. 10), which showed GAG secretion. As HA is a nonsulfated GAG, it stains blue in alcian blue staining. Low amounts of HA in the scaffold can be easily distinguished from newly deposited ECM by the chondrocytes by comparing alcian blue staining at 1 (Fig. $10A_1$–$A_{35}$) with staining at later time intervals. At day 1, chondrocytes did not attach to the walls of CHT scaffolds, whereas in CHT/HA scaffolds, the cells attached to walls, forming small aggregates. At day 14, in CHT/5HA scaffolds (Fig. $9C_{14}$ and Fig. $10C_{14}$), it was interesting to note that most chondrocytes agglomerated to form very large aggregates adherent to the scaffolds. The aggregates were located on the superficial area. Hardly any penetration of cells in the scaffolds was observed. These events were also reported by Zhao *et al.*[43] CHT/1HA and CHT/5HA showed enhanced cell–material interactions and ECM production, with enhanced GAG production (Figs. 9 and 10). At day 35, CHT/5HA scaffolds showed better cell dispersion and higher ECM production and GAG deposition when compared with the other formulations. Chondrocytes seeded in CHT scaffolds, even at day 35, remained in small aggregates (Fig. $9A_{35}$ and Fig. $10A_{35}$).

Enhanced cartilage tissue formation can be also qualitatively detected by SEM analysis (Fig. 11). At day 1, chondrocytes were in aggregates in all specimens, but at day 14 they were better spread and attached. At days 14 and 21, improved chondrocyte dispersion could be noticed in CHT/1HA and CHT/5HA scaffolds. In all specimens, lacunae

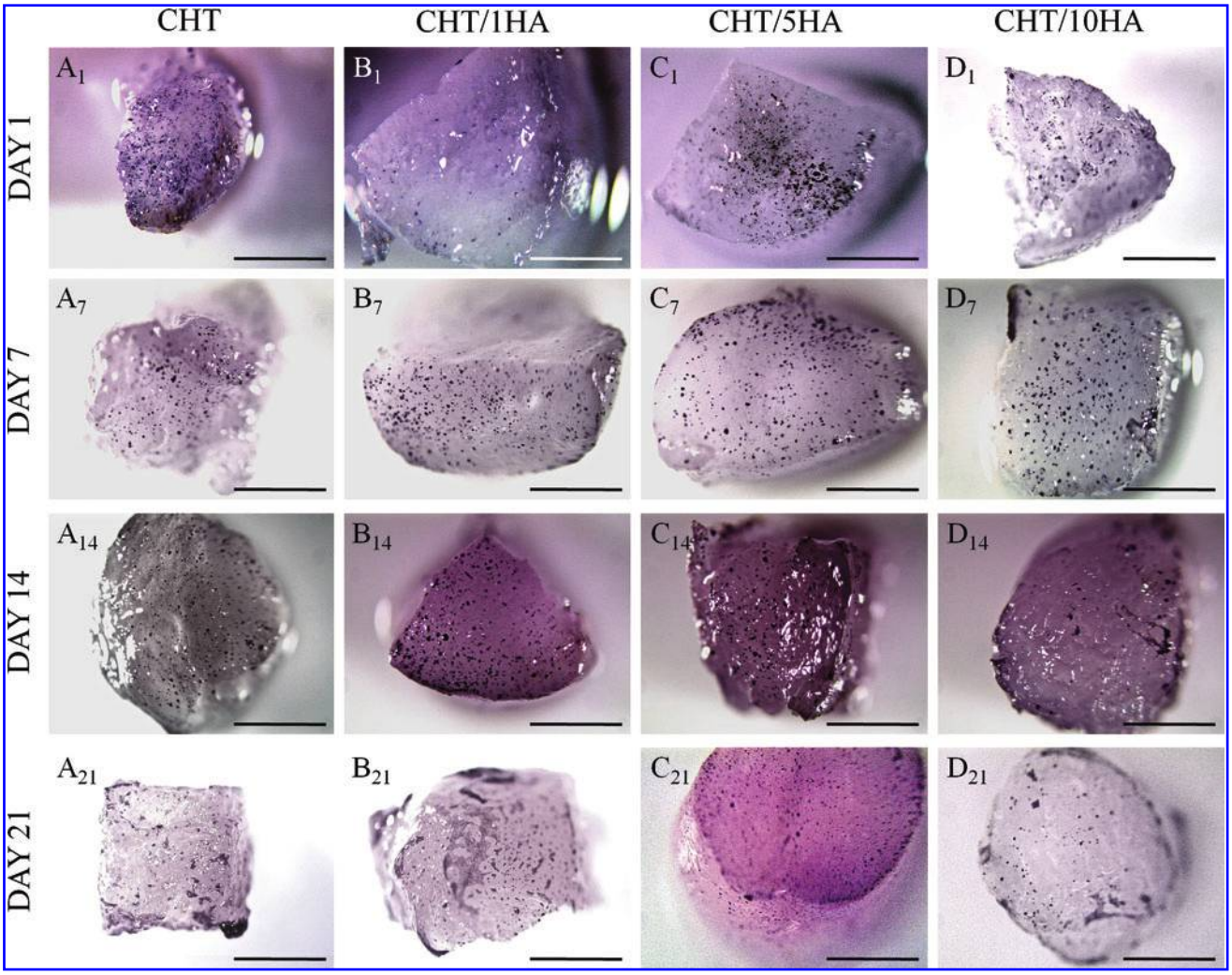


**FIG. 7.** MTT assay results of chondrocytes at passage 3 in proliferation medium seeded on CHT/HA scaffolds at days 1, 7, 14, and 21 ($n=3$). Metabolic active cells were stained dark purple. Letters **A–D** correspond to each of the four scaffold's formulations, namely CHT, CHT/1HA, CHT/5HA or CHT/10HA, respectively. The subscripts indicate the time period. Original magnification is ×7.5. Scale bar is 3 cm. Color images available online at www.liebertonline.com/tec

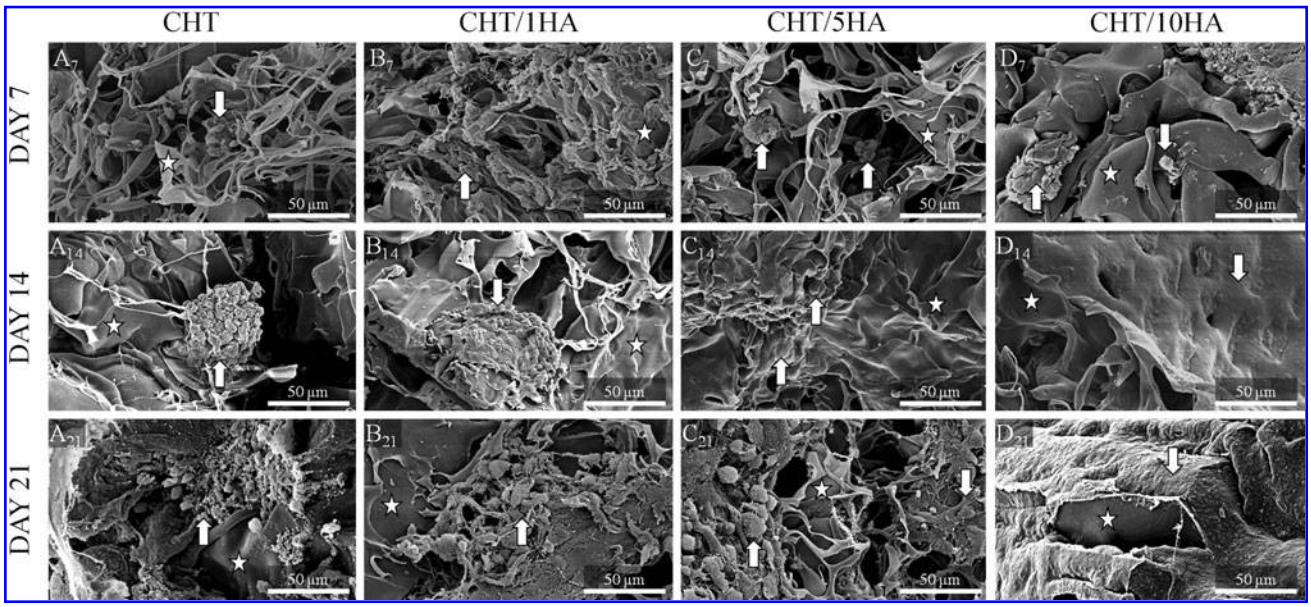


**FIG. 8.** SEM micrographs (10 kV) of CHT/HA scaffolds seeded with articular bovine chondrocytes at passage 3 in proliferation medium ($n=2$). Letters **A–D** correspond to each of the four scaffold's formulations, namely CHT, CHT/1HA, CHT/5HA or CHT/10HA, respectively. The subscripts indicate the time period. Original magnification is ×500. Scale bar is 50 µm. Arrows point to chondrocytes and/or cartilage extracellular matrix deposition and stars indicate scaffold material.

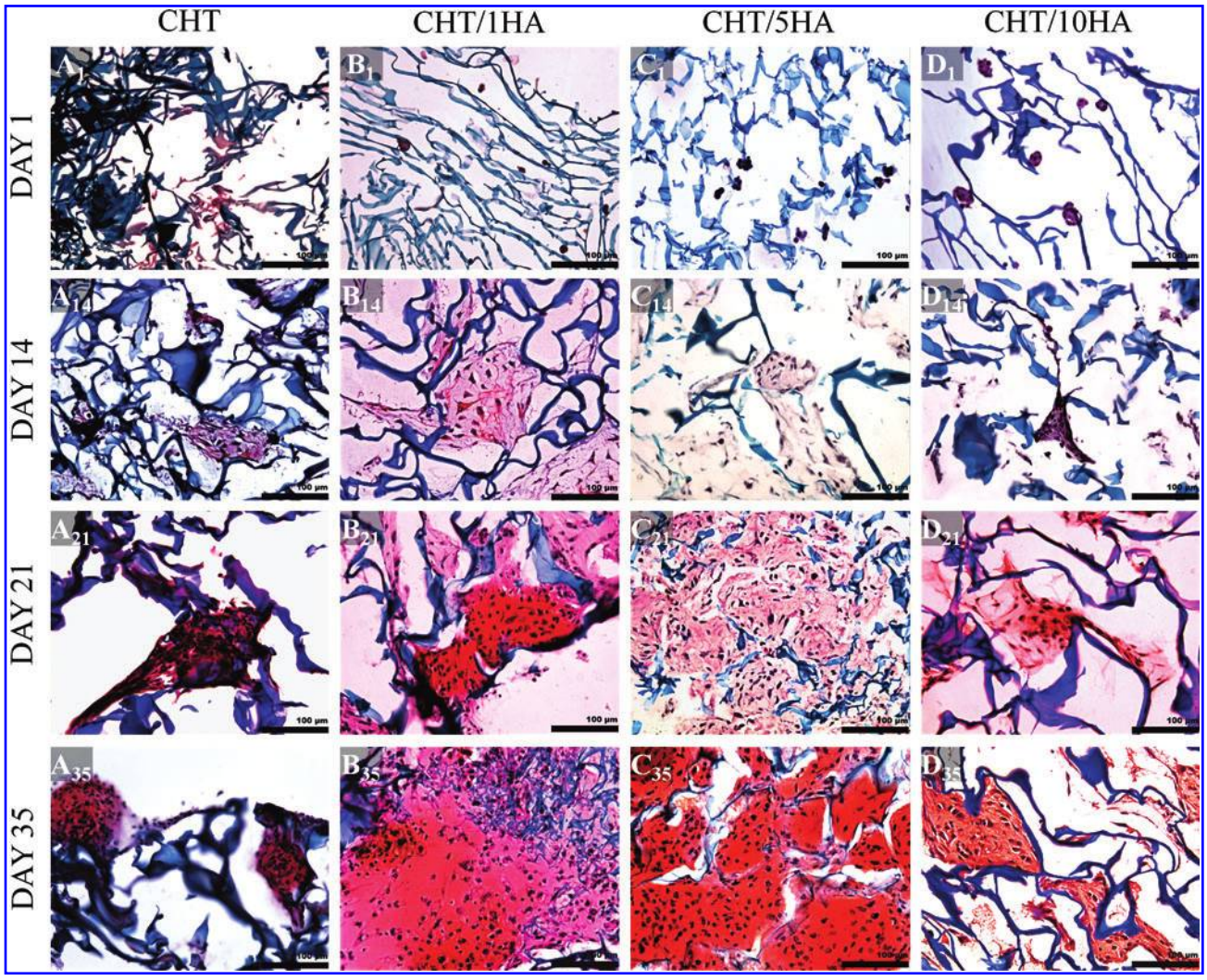


**FIG. 9.** Histological cross-sections show glycosaminoglycan (GAG) deposition (stained red) in CHT/HA scaffolds by safranin-O staining at 1, 14, 21, and 35 days of chondrocyte culture in differentiation medium ($n=2$). Letters **A–D** correspond to each of the four scaffold's formulations, namely CHT, CHT/1HA, CHT/5HA or CHT/10HA, respectively. Subscripts indicate time intervals. Scale bar is 100 μm. Color images available online at www.liebertonline.com/tec

formation was seen in the matrix surrounding the chondrocytes. The morphology of these lacunas shows similarities to natural cartilage.

Chondrogenic activity evaluation. It is known that when chondrocytes maintain their natural spherical shape they produce more GAGs and higher collagen type II versus collagen type I ratio.[44–46] Cell proliferation and ECM formation were quantified by DNA and GAG assays, respectively. In GAG quantification assay (Fig. 12a), the incorporation of HA seemed to initiate an earlier GAG deposition, particularly at day 14 for CHT/1HA and CHT/5HA scaffolds. Results showed that the incorporation of HA seemed to favor GAG deposition, because at day 35 all the scaffolds containing HA had more GAG deposition when compared with CHT scaffolds. For DNA quantification assay (Fig. 12b), CHT/5HA had the highest amount of DNA at day 14. However, at day 35, CHT/1HA scaffolds significantly supported a higher amount of cells when compared with other formulations.

A higher value of GAG/DNA ratio indicates a higher degree of differentiation of the cells.[47] For GAG/DNA ratio (Fig. 12c), at day 35, scaffolds with higher amount of HA (CHT/5HA and CHT/10HA) induced a higher ratio. Although CHT/1HA had the highest amount of cells in DNA quantification, CHT/5HA had the highest GAG versus DNA ratio. This may imply that CHT/5HA scaffolds are the formulation that most favors cartilage ECM production, rendering them attractive for cartilage TE.

### *Physicochemical effects of CHT/HA scaffolds on cartilage regeneration*

The key challenge for biomedical researchers is how to design and control material properties to achieve a specific biological response.[48] It has been well established that the physicochemical properties of materials can regulate biological responses, such as differentiation of stem cells,[49] proliferation of fibroblasts,[50] gene delivery,[51] and cell death.[52]

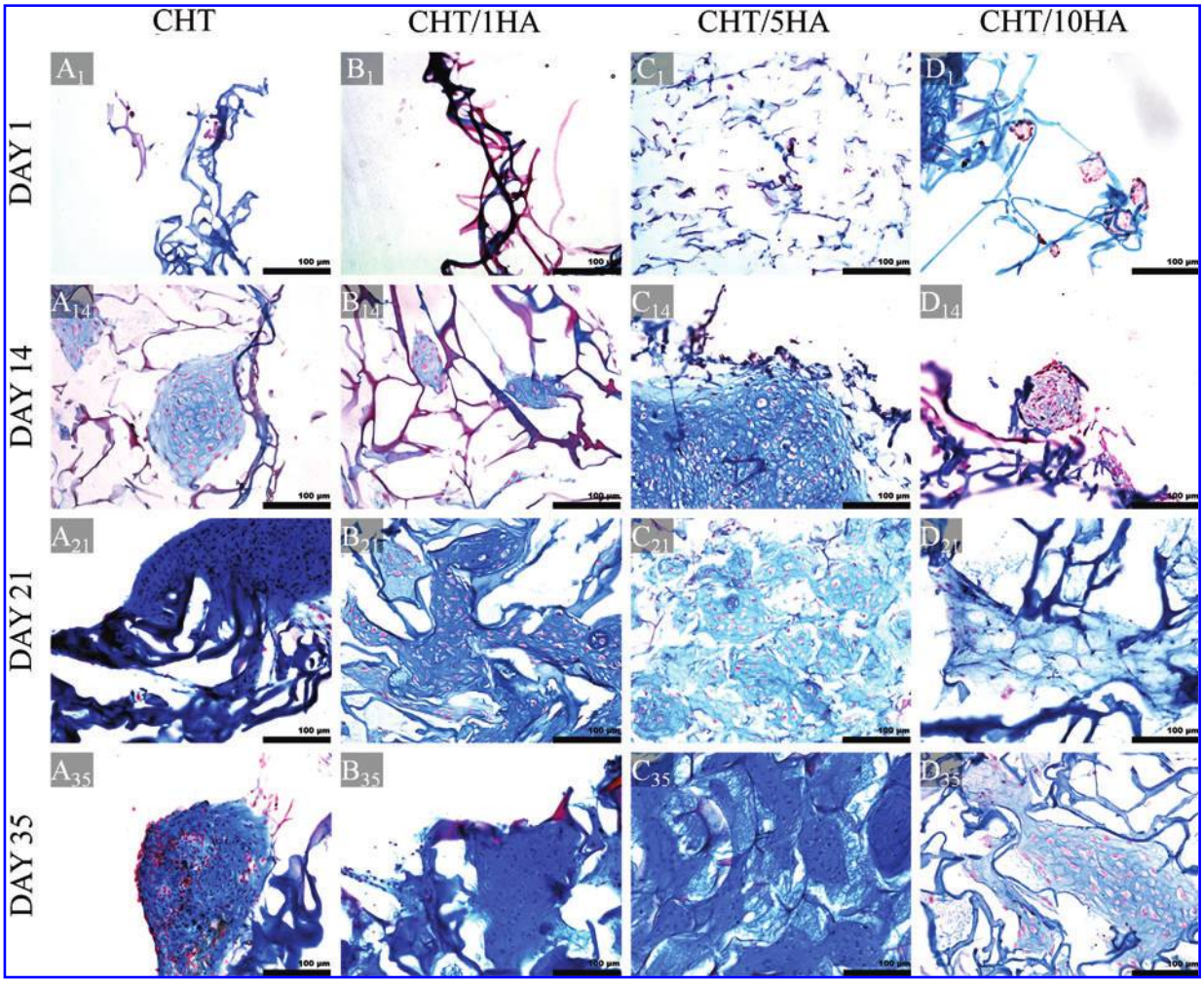


**FIG. 10.** Histological cross-sections show GAG deposition (stained blue) in CHT/HA scaffolds by alcian blue staining at 1, 14, 21, and 35 days of chondrocyte culture in differentiation medium ($n=2$). Letters **A–D** correspond to each of the four scaffold's formulations, namely CHT, CHT/1HA, CHT/5HA or CHT/10HA, respectively. Subscripts indicate time intervals. Scale bar is 100 µm. Color images available online at www.liebertonline.com/tec

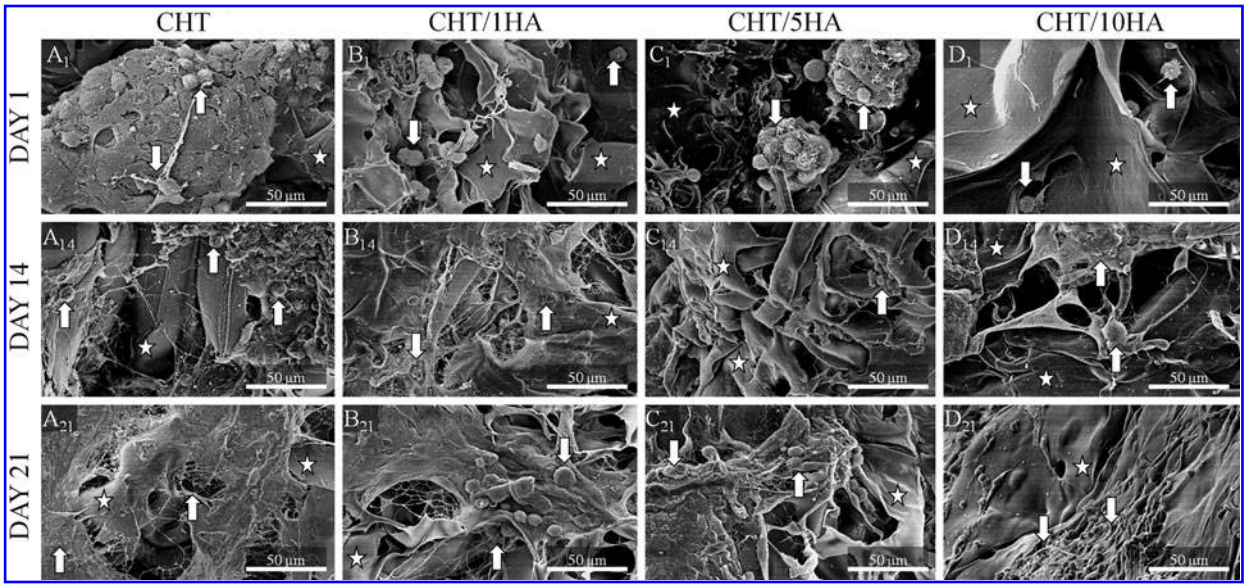


**FIG. 11.** SEM micrographs (10 kV) of CHT/HA scaffolds seeded with articular bovine chondrocytes at passage 1 in differentiation medium ($n=2$). Letters **A–D** correspond to each of the four scaffold's formulations, namely CHT, CHT/1HA, CHT/5HA or CHT/10HA, respectively. The subscripts indicate the time period. Original magnification is ×500. Scale bar is 50 µm. Arrows point to chondrocytes and/or cartilage extracellular matrix deposition and stars indicate scaffold material.

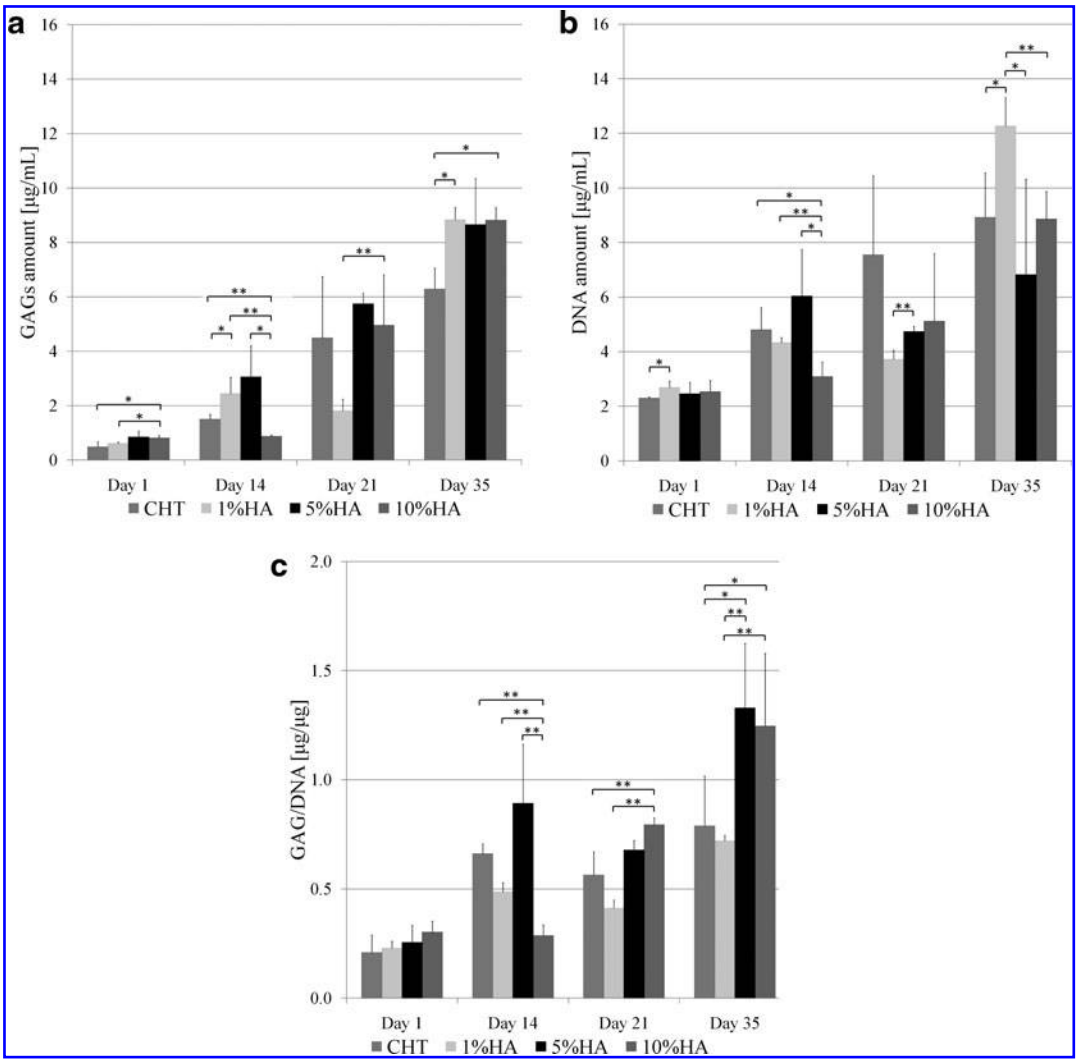


**FIG. 12.** GAG and DNA assays on CHT/HA scaffolds at 1, 14, 21, and 35 days of culture: **(a)** GAG assay, **(b)** DNA assay, **(c)** GAGs per DNA ratio. Values are reported as mean ± standard deviation ($n = 3$). Significant differences for $^{*}p \leq 0.05$ and $^{**}p \leq 0.01$ were found.

CHT/1HA and CHT/5HA scaffolds exhibited a uniform pore network with high porosity (Fig. 1) and a homogeneous polymer dispersion (Fig. 3), rendering them suitable for bovine chondrocyte culture. The pore configuration allowed cellular infiltration into the inner pores of the scaffolds (Fig. 8). On the other hand, CHT and CHT/10HA scaffolds had a very irregular pore network configuration with closed pores. Consequently, in these scaffolds, the adhesion and proliferation of chondrocytes were jeopardized when compared with the other formulations. The scaffolds' high water uptake ability (Fig. 4) allowed the chondrocyte medium to reach the interior pores of the scaffolds. Consequently, diffusion and exchange of nutrients and waste throughout the scaffolds were ensured, allowing cells to proliferate and be metabolically active (Figs. 6 and 7).

Besides appropriate pore network and water uptake ability, CHT/1HA and, especially, CHT/5HA had an improved GAG dispersion and deposition (Figs. 9 and 10). Additionally, the two referred formulations had similar compressive modulus. Hence, physical and chemical factors seem to simultaneously influence the biological outcome. Cartilage regeneration seemed to be favored simultaneously by chemical aspects, that is, intermediate amounts of HA (1% and 5%), and also by physical aspects, that is, the referred scaffold formulations also have similar compressive modulus and a uniform pore network configuration. Therefore, in this case scenario, it is not possible to distinguish case by case the detailed mechanisms of how physical properties affect the biological performance of the CHT/HA scaffolds. Despite this unclear contribution of each parameter, the results obtained in our study are not compromised.

## Conclusions

The incorporation of HA up to a concentration of 5% in CHT scaffolds improved the physicochemical properties and biological properties of CHT scaffolds. It enhanced pore network configuration and increased pore size, swelling ratio, and degradation rate when compared with pure CHT scaffolds. Higher concentrations of HA resulted in heterogeneous blends with irregular and collapsed pore networks, particularly CHT/5HA scaffolds favored chondrocyte adhesion, cell

proliferation, and cartilage matrix production when compared with pure CHT scaffolds and other CHT/HA blends.

The biological outcome of CHT/HA scaffolds seems to be influenced by physicochemical factors, such as polymer dispersion, pore network configuration, pore size, water uptake ability, and mechanical strength. However, other studies are required to elucidate case by case the dependence of biological response on physical properties and to categorize the relative weight of different physical and chemical factors.

Our results suggest that the freeze-dried scaffolds of CHT and HA could have potential use in the regeneration of cartilaginous lesions caused by various joint diseases, including osteoarthritis and rheumatoid arthritis.

### Disclosure Statement

No competing financial interests exist.

### References


1. Wu, S.C., Chang, J.K., Wang, C.K., Wang, C.J., and Ho, M.L. Enhancement of chondrogenesis of human adipose derived stem cells in a hyaluronan-enriched microenvironment. Biomaterials **31,** 631, 2010.
2. Bobic, V., and Noble, J. Articular cartilage, to repair or not to repair. J Bone Joint Surg Br **82,** 165, 2000.
3. Temenoff, J.S., and Mikos, A.G. Review: tissue engineering for regeneration of articular cartilage. Biomaterials **21,** 431, 2000.
4. Gobbi, A., Nunag, P., and Malinowski, K. Treatment of full thickness chondral lesions of the knee with microfracture in a group of athletes. Knee Surg Sports Traumatol Arthrosc **13,** 213, 2005.
5. Lee, J., Lee, J.Y., Lee, E., and Son, Y. Newborn calf serum retards loss of the chondrocytic phenotype during *in vitro* cell expansion. J Tissue Eng Regen Med **6,** 229, 2009.
6. Lin, Y.C., Tan, F.J., Marra, K.G., Jan, S.S., and Liu, D.C. Synthesis and characterization of collagen/hyaluronan/chitosan composite sponges for potential biomedical applications. Acta Biomater **5,** 2591, 2009.
7. Mano, J.F., and Reis, R.L. Osteochondral defects: present situation and tissue engineering approaches. J Tissue Eng Regen Med **1,** 261, 2007.
8. Chen, G., Ushida, T., and Tateishi, T. Scaffold design for tissue engineering. Macromol Biosci **2,** 67, 2002.
9. Goldring, M.B., Tsuchimochi, K., and Ijiri, K. The control of chondrogenesis. J Cell Biochem **97,** 33, 2006.
10. Yoo, H.S., Lee, E.A., Yoon, J.J., and Park, T.G. Hyaluronic acid modified biodegradable scaffolds for cartilage tissue engineering. Biomaterials **26,** 1925, 2005.
11. Kim, I.Y., Seo, S.J., Moon, H.S., Yoo, M.K., Park, I.Y., Kim, B.C., and Cho, C.S. Chitosan and its derivatives for tissue engineering applications. Biotechnol Adv **26,** 1, 2008.
12. Ghosh, P., and Guidolin, D. Intra-articular hyaluronan therapy in osteoarthritis. Semin Arthritis Rheum **32,** 10, 2002.
13. Ren, Y.J., Zhou, Z.Y., Liu, B.F., Xu, Q.Y., and Cui, F.Z. Preparation and characterization of fibroin/hyaluronic acid composite scaffold. Int J Biol Macromol **44,** 372, 2009.
14. Tian, W.M., Hou, S.P., Ma, J., Zhang, C.L., Xu, Q.Y., and Lee, I.S. Hyaluronic acid–poly-D-lysine-based three-dimensional hydrogel for traumatic brain injury. Tissue Eng **11,** 513, 2005.
15. Oyarzun-Ampuero, F.A., Brea, J., Loza, M.I., Torres, D., and Alonso, M.J. Chitosan-hyaluronic acid nanoparticles loaded with heparin for the treatment of asthma. Int J Pharm **381,** 122, 2009.
16. Tan, H., Wu, J., Lao, L., and Gao, C. Gelatin/chitosan/hyaluronan scaffold integrated with PLGA microspheres for cartilage tissue engineering. Acta Biomater **5,** 328, 2009.
17. Martino, A.D., Sittinger, M., and Risbud, M.V. Chitosan: a versatile biopolymer for orthopaedic tissue-engineering. Biomaterials **26,** 5983, 2005.
18. Kim, S.E., Park, J.H., Cho, Y.W., Chung, H., Jeong, S.Y., Lee, E.B., and Kwon, I.C. Porous chitosan scaffold containing microspheres loaded with transforming growth factor-β1: implications for cartilage tissue engineering. J Control Release **91,** 365, 2003.
19. Oliveira, J.M., Rodrigues, M.T., Silva, S.S., Malafaya, P.B., Gomes, M.E., Viegas, C.A., Dias, I.R., Azevedo, J.T., Mano, J.F., and Reis, R.L. Novel hydroxyapatite/chitosan bilayered scaffold for osteochondral tissue-engineering applications: scaffold design and its performance when seeded with goat bone marrow stromal cells. Biomaterials **27,** 6123, 2006.
20. Nge, T.T., Nogi, M., Yano, H., and Sugiyama, J. Microstructure and mechanical properties of bacterial cellulose/chitosan porous scaffold. Cellulose **17,** 349, 2010.
21. Tan, H., Chu, C.R., Payne, K.A., and Marra, K.G. Injectable *in situ* forming biodegradable chitosan-hyaluronic acid based hydrogels for cartilage tissue engineering. Biomaterials **30,** 2499, 2009.
22. Yamane, S., Iwasaki, N., Majima, T., Funakoshi, T., Masuko, T., Harada, K., Minami, A., Monde, K., and Nishimura, S.I. Feasibility of chitosan-based hyaluronic acid hybrid biomaterial for a novel scaffold in cartilage tissue engineering. Biomaterials **26,** 611, 2005.
23. Yamane, S., Iwasaki, N., Kasahara, Y., Harada, K., Majima, T., Monde, K., Nishimura, S.I., and Minami, A. Effect of pore size on *in vitro* cartilage formation using chitosan-based hyaluronic acid hybrid polymer fibers. J Biomed Mater Res A **81A,** 587, 2006.
24. Hsu, S.H., Whu, S.W., Hsieh, S.C., Tsai, C.L., Chen, D.C., and Tan, T.S. Evaluation of chitosan-alginate-hyaluronate complexes modified by an RGD-containing protein as tissue engineering scaffolds for cartilage regeneration. Artif Organs **28,** 693, 2004.
25. Chen, J.P., and Cheng, T.H. Preparation and evaluation of thermo-reversible copolymer hydrogels containing chitosan and hyaluronic acid as injectable cell carriers. Polymer **50,** 107, 2009.
26. Chung, T.W., Yang, J., Akaike, T., Cho, K.Y., Nah, J.W., Kim, S., II, and Cho, C.S. Preparation of alginate/galactosylated chitosan scaffold for hepatocyte attachment. Biomaterials **23,** 2827, 2002.
27. Ji, Y., Ghosh, K., Shu, X.Z., Li, B., Sokolov, J.C., Prestwic, G.D., Clark, R.A.F., and Rafailovich, M.H. Electrospun three-dimensional hyaluronic acid nanofibrous scaffolds. Biomaterials **27,** 3782, 2006.
28. Antunes, J.C., Oliveira, J.M., Reis, R.L., Soria, J.M., Goméz-Ribelles, J.L., and Mano, J.F. Novel poly (L-lactic acid)/hyaluronic acid macroporous hybrid scaffolds: characterization and assessment of cytotoxicity. J Biomed Mater Res A **94,** 856, 2010.
29. Greenwald, R.A., Josephson, A.S., Diamond, H.S., and Tsang, A. Human cartilage lysozyme. J Clin Invest **51,** 2264, 1972.
30. Jin, R., Moreira-Teixeira, L.S., Krouwels, A., Dijkstra, P.J., van Blitterswijk, C.A., Karperien, M., and Feijen, J. Synthesis and characterization of hyaluronic acid-peg hydrogels via Michael addition: an injectable biomaterial for cartilage repair. Acta Biomater **6,** 1968, 2010.

31. Fan, J., Shang, Y., Yuan, Y., and Yang, J. Preparation and characterization of chitosan/galactosylated hyaluronic acid scaffolds for primary hepatocytes culture. J Mater Sci Mater Med **21,** 319, 2010.
32. Mao, J.S., Liu, H.F., Yin, Y.J., and Yao, K.D. The properties of chitosan–gelatin membranes and scaffolds modified with hyaluronic acid by different methods. Biomaterials **24,** 1621, 2003.
33. O'Brien, F.J., Harley, B.A., Yannas, I.V., and Gibson, L. Influence of freezing rate on pore structure in freeze-dried collagen–GAG scaffolds. Biomaterials **25,** 1077, 2004.
34. Korhonen, R.K., Laasanen, M.S., Töyräs, J., Rieppo, J., Hirvonen, J., Helminen, H.J., and Jurvelin, J.S. Comparison of the equilibrium response of articular cartilage in unconfined compression, confined compression and indentation. J Biomech **35,** 903, 2002.
35. Pangburn, S.H., Trescony, P.V., and Heller, J. Lysozyme degradation of partially deacetylated chitin, its films and hydrogels. Biomaterials **3,** 105, 1982.
36. Tomihata, K., and Ikada, Y. *In vitro* and *in vivo* degradation of films of chitin and its deacetylated derivatives. Biomaterials **18,** 567, 1997.
37. Lee, K.Y., Ha, W.S., and Park, W.H. Blood compatibility and biodegradability of partially N-acylated chitosan derivatives. Biomaterials **16,** 1211, 1995.
38. Hirano, S., Tsuchida, H., and Nagao, N. N-acetylation in chitosan and the rate of its enzymatic hydrolysis. Biomaterials **10,** 574, 1989.
39. Fraser, J.R.E., Laurent, T.C., and Laurent, U.B.G. Hyaluronan: its nature, distribution, functions and turnover. J Intern Med **242,** 27, 1997.
40. Nordtveit, R.J., Värum, K.M., and Smidsrød, O. Degradation of partially N-acetylated chitosans with hen egg white and human lysozyme. Carbohydr Polym **29,** 163, 1996.
41. Telmel, A., Kazokoglu, H., and Taga, Y. Tear lysozyme levels in contact lens wearers. Ann Ophthalmol **23,** 191, 1991.
42. Von der Mark, K., Gauss, V., von der Mark, H., and Muller, P. Relationship between cell shape and type of collagen synthesized as chondrocytes lose their cartilage phenotype in culture. Nature **267,** 531, 1977.
43. Zhao, K., Deng, Y., Chen, J.C., and Chen, G.Q. Polyhydroxyalkanoate (PHA) scaffolds with good mechanical properties and biocompatibility. Biomaterials **24,** 1041, 2003.
44. Woodfield, T.B.F., Miot, S., Martin, I., van Blitterswijk, C.A., and Riesle, J. The regulation of expanded human nasal chondrocyte re-differentiation capacity by substrate composition and gas plasma surface modification. Biomaterials **27,** 1043, 2006.
45. Miot, S., Woodfield, T.B.F., Daniels, A.U., Suetterlin, R., Peterschmitt, I., Heberer, M., van Blitterswijk, C.A., Riesle, J., and Martin, I. Effects of scaffold composition and architecture on human nasal chondrocyte redifferentiation and cartilaginous matrix deposition. Biomaterials **26,** 2479, 2005.
46. Barry, J.J., Gidda, H.S., Scotchford, C.A., and Howdle, S.M. Porous methacrylate scaffolds: supercritical fluid fabrication and *in vitro* chondrocyte responses. Biomaterials **25,** 3559, 2004.
47. Moroni, L., Schotel, R., Hamann, D., de Wijn, J.R., and van Blitterswijk, C.A. 3D fiber-deposited electrospun integrated scaffolds enhance cartilage tissue formation. Adv Funct Mater **18,** 53, 2008.
48. Mitragotri, S., and Lahann, J. Physical approaches to biomaterial design. Nat Mater **8,** 15, 2009.
49. Graziano, A., d'Aquino, R., Cusella-De Angelis, M.G., Francesco, F., Giordano, A., Laino, G., Piattelli, A., Traini, T., Rosa, A., and Papaccio, G. Scaffold's surface geometry significantly affects human stem cell bone tissue engineering. J Cell Physiol **214,** 166, 2008.
50. Milner, K.R., and Siedlecki, C.A. Submicron poly(L-lactic acid) pillars affect fibroblast adhesion and proliferation. J Biomed Mater Res A **82,** 80, 2007.
51. Shen, H., Tan, J., and Saltzman, W.M. Surface-mediated gene transfer from nanocomposites of controlled texture. Nat Mater **3,** 569, 2004.
52. Chen, C.S., Mrksich, M., Huang, S., Whitesides, G.M., and Ingber, D.E. Geometric control of cell life and death. Science **276,** 1425, 1997.

Address correspondence to:
*João F. Mano, Ph.D.*
*3B's Research Group—Biomaterials, Biodegradables, and Biomimetics*
*Headquarters of the European Institute of Excellence on Tissue Engineering and Regenerative Medicine*
*University of Minho*
*AvePark*
*Zona Industrial da Gandra*
*S. Cláudio do Barco*
*Guimarães 4806-909*
*Portugal*

*E-mail:* jmano@dep.uminho.pt

*Received: August 9, 2010*
*Accepted: March 7, 2011*
*Online Publication Date: April 22, 2011*

**This article has been cited by:**


1. Anna G. Mitsak, Andrew M. Dunn, Scott J. Hollister. 2012. Mechanical characterization and non-linear elastic modeling of poly(glycerol sebacate) for soft tissue engineering. *Journal of the Mechanical Behavior of Biomedical Materials* **11**, 3-15. [CrossRef]
2. Amos Matsiko, Tanya J. Levingstone, Fergal J. O'Brien, John P. Gleeson. 2012. Addition of hyaluronic acid improves cellular infiltration and promotes early-stage chondrogenesis in a collagen-based scaffold for cartilage tissue engineering. *Journal of the Mechanical Behavior of Biomedical Materials* **11**, 41-52. [CrossRef]
3. Amanda N. Renth , Michael S. Detamore . Leveraging "Raw Materials" as Building Blocks and Bioactive Signals in Regenerative Medicine. *Tissue Engineering Part B: Reviews*, ahead of print. [Abstract] [Full Text HTML] [Full Text PDF] [Full Text PDF with Links]
4. Nandana Bhardwaj, Subhas C. Kundu. 2012. Chondrogenic differentiation of rat MSCs on porous scaffolds of silk fibroin/chitosan blends. *Biomaterials* . [CrossRef]
5. Christiane L. Salgado, Mariana B. Oliveira, João F. Mano. 2012. Combinatorial cell–3D biomaterials cytocompatibility screening for tissue engineering using bioinspired superhydrophobic substrates. *Integrative Biology* . [CrossRef]
6. Dunia Mercedes García Cruz, Manuel Salmerón-Sánchez, José Luis Gómez-Ribelles. 2012. Stirred flow bioreactor modulates chondrocyte growth and extracellular matrix biosynthesis in chitosan scaffolds. *Journal of Biomedical Materials Research Part A* n/a-n/a. [CrossRef]
7. GyuHyun Jin, GeunHyung Kim. 2012. Multi-layered polycaprolactone–alginate–fucoidan biocomposites supplemented with controlled release of fucoidan for bone tissue regeneration: fabrication, physical properties, and cellular activities. *Soft Matter* **8**:23, 6264. [CrossRef]